

## COMPARISON BETWEEN CLUSTER MONTE CARLO ALGORITHMS IN THE ISING MODEL

ULI WOLFF

*Institut für Theoretische Physik, Universität Kiel, D-2300 Kiel, FRG*

Received 3 July 1989

We report autocorrelation times for the Swendsen–Wang algorithm and for a recently proposed single cluster variant in the 2D and 3D Ising models at criticality. The new algorithm decorrelates faster in all cases and gains about an order of magnitude on a  $64^3$  lattice. Critical slowing down is practically negligible and possibly completely absent in three dimensions. Results on static properties of the 3D model are consistent with published data.

Among the attempts to circumvent critical slowing-down in simulations of field theories and critical systems a line of developments related to percolation and initiated by Swendsen and Wang (SW) [1] has been very successful recently. While the original SW proposal works for Potts spins only, our recent generalization [2] has been applied to the  $x$ - $y$  model [3] and to the O(3) nonlinear  $\sigma$ -model [4] in two dimensions with the result of no detectable slowing down and further advantages related to variance reduction. Apart from the generalization to continuous spins our proposal [2] also modifies the SW algorithm in another way: the single cluster (1C) construction (see below). Consequently the new 1C algorithm *does not coincide* with SW even for Potts models. Here we study two-state Potts (=Ising) models to evaluate the effect of the 1C variation in isolation. This complements recent studies [5,6] where the combination of continuous spins with the original SW cluster decomposition has also been found to drastically reduce or eliminate slowing down. The results of ref. [5] combined with ref. [1] or with the present study actually imply that the SW cluster construction leads to a smaller dynamical exponent  $z$  for continuous spins than for Ising spins. The latter are thus “harder” to simulate than O( $n$ )  $\sigma$ -models with  $n > 1$ .

The SW and 1C algorithms for an Ising model

$$Z = \sum_{\{s_x = \pm 1\}} \exp \left( \beta \sum_{x\mu} s_x s_{x+\mu} \right) \quad (1)$$

with spins  $s_x$  at the sites  $x$  of a  $d$ -dimensional hyper-torus of  $L^d$  sites are most easily described in words: For given spins  $\{s_x\}$  one activates bonds  $x\mu$  (links) with probability

$$p_{x\mu}[s] = \delta_{s_x, s_{x+\mu}} [1 - \exp(-2\beta)] . \quad (2)$$

Active bonds connect pairs of sites and lead to a decomposition of the set  $\mathcal{A}$  of all sites into bond percolation clusters

$$\mathcal{A} = \bigcup_{i=1}^{N_c} c_i . \quad (3)$$

The two algorithms differ now in the way in which a cluster  $C$  is formed of spins that are flipped to complete the update. SW effectively take the union  $C_{SW}$  of a subset of the components  $c_i$  where each individual component is included with probability  $\frac{1}{2}$ . The 1C algorithm may be implemented pictorially as follows: Throw a dart on the lattice that hits each site with the same probability (absolute beginner!). The site  $x_0$  that is picked belongs to a component  $c_{i_0}$  which we take for  $C_{1C} = c_{i_0}$ . In the practical realization of the 1C algorithm one actually proceeds slightly differently: We *first* pick  $x_0$  and then construct *only* the cluster  $C_{1C}$  connected to it. This requires only of the order of  $|C_{1C}|$  operations as opposed to  $|A| = L^d$ , where  $|C_{1C}|$  is the mass (# of sites) of the cluster. This is a very important difference when the correlation length is finite, and typical clusters are small compared to the volume. Clearly, the 1C method prefers to flip large coherently formed clusters with a bias

proportional to their mass. It can be shown [4,2] that their average mass equals the magnetic susceptibility

$$\langle |C_{1C}| \rangle = \chi = L^{-d} \left\langle \left( \sum_x s_x \right)^2 \right\rangle. \tag{4}$$

For SW we trivially have

$$\langle |C_{SW}| \rangle = |A|/2. \tag{5}$$

For the mass of a typical coherent component  $c_i$  in  $C_{SW}$  we found little volume dependence at (pseudo) criticality with values settling around

$$\begin{aligned} \langle |c_i| \rangle &\approx 7.8 \quad \text{for } d=2, \\ &\approx 3.2 \quad \text{for } d=3, \end{aligned} \tag{6}$$

from above for large volumes. Eq. (4), which holds independently of  $\beta$ , may be interpreted as suggesting that the scale of equilibrium physics and the typical size of 1C updating steps are closely related – intuitively a prerequisite to eliminate critical slowing down. We find the SW case more difficult to interpret and compared the behavior of both algorithms in a series of numerical experiments.

Before we come to our results, we would like to give details on how we determined autocorrelation times. Imagine successive estimates  $O_i$  for a physical quantity  $O$  coming from some Monte Carlo process. The normalized autocorrelation function  $\rho$  is given by

$$\rho(t) = \frac{\langle O_i O_{i+t} \rangle - \langle O \rangle^2}{\langle O^2 \rangle - \langle O \rangle^2}, \tag{7}$$

and will be estimated from our data. The integrated autocorrelation time

$$\tau = \frac{1}{2} \sum_{t=-\infty}^{\infty} \rho(t) \tag{8}$$

is precisely the quantity required to estimate errors  $\Sigma_N$  for  $O$  in a Monte Carlo experiment with  $N$  correlated measurements,

$$\Sigma_N^2 = (\langle O^2 \rangle - \langle O \rangle^2) 2\tau/N. \tag{9}$$

As discussed in ref. [7] one has to appropriately truncate the sum in (8) to obtain  $\tau$  from the data as otherwise noisy contributions from large separations make the variance of this estimate diverge. For a truncation window  $W$  we use the estimator

$$\tau(W) = \frac{1}{2} + \sum_{t=1}^{W-1} \rho(t) + R(W), \tag{10}$$

with the remainder

$$\begin{aligned} R(W) &= \rho(W) \frac{1}{1-\kappa(W)}, \\ \kappa(W) &= \frac{\rho(W)}{\rho(W-1)}. \end{aligned} \tag{11}$$

In fig. 1 we show data for  $O=\chi$  from our 1C simulation on  $64^3$ . Clearly estimates (10) (dots) have converged for  $W \approx \tau$ . In ref. [7] the remainder  $R$  is neglected, and we see that for a  $W$  of several  $\tau$  the same value is approached from below. The exponential correlation time  $\tau^{\text{exp}}(W) = -1/\log \kappa(W)$  would clearly be hard to extrapolate. We developed a formula for the error  $\sigma_N(W)$  of  $\tau(W)$  in (10) based on similar approximations as were used in ref. [7]. Most importantly, the four-point autocorrelation function is approximated by its disconnected part. This leads to

$$\begin{aligned} \sigma_N^2(W) &= \frac{4}{N} \left[ \tau^2 \left( W - \frac{1}{2} + \frac{1+\kappa}{1-\kappa} \right) \right. \\ &\quad \left. + \frac{\kappa X}{(1-\kappa)^2} + \frac{\kappa^2 Y}{(1-\kappa)^4} \right], \end{aligned} \tag{12}$$

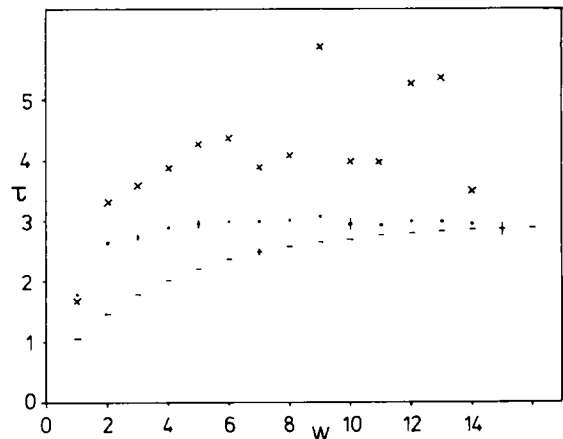


Fig. 1 Autocorrelation times for the susceptibility  $\chi$  of the critical Ising model on a  $64^3$  lattice. Measurements are separated by 20 1C update steps flipping an average of  $\approx 41\%$  of all spins. Crosses are estimates of the exponential autocorrelation time  $\tau^{\text{exp}}$ , dots give  $\tau^{\text{integrated}}$  obtained with (10) and (12), and horizontal bars correspond to the method of ref. [7]. Errors drawn are  $\pm \sigma$

where all arguments on the RHS are  $W$ , and we introduced

$$X(W) = \frac{1}{2} + \sum_{t=1}^{W-1} \rho(t)^2,$$

$$Y(W) = \frac{1}{2} \sum_{t=1}^{W-1} [\rho(t) - \rho(t-1)]^2. \quad (13)$$

These errors are displayed in fig. 1 for some sample  $W$  values. We found them quite consistent with the scattering among multiple runs, with the oscillations around the plateau in  $W$ , and with ref. [7] for large enough  $W$ . We think, however, that the present method makes particularly efficient use of given autocorrelation data up to some time separation. The outcomes for all our measurements looked qualitatively similar to fig. 1 and hence were easy to extrapolate.

In two dimensions we chose the self-dual value  $\beta = \frac{1}{2} \log(1 + \sqrt{2})$  for our simulations, and in  $d=3$  we took  $\beta = 0.22165$  obtained with the Santa Barbara Ising processor [8]. Our results on the magnetic susceptibility and the nearest neighbor correlation  $E$  as well as (integrated) autocorrelation times are summarized in table 1. In the last two columns we quote autocorrelation times from independent SW runs. They refer to the natural unit of an SW sweep, i.e. one passage through the lattice generating a complete cluster decomposition and new spins on the clusters. For the 1C runs we first obtained correlation times  $\bar{\tau}$  among measurements separated by some convenient fixed number  $m$  of 1C steps [2]. Only after the run we convert  $\bar{\tau}$  to  $\tau_{1C}$ ,

$$\tau_{1C} = \bar{\tau} \frac{m \langle |C_{1C}| \rangle}{L^d}, \quad (14)$$

which refers to flips per spin. We found the average CPU time required to produce and flip the (typically) large 1C clusters (see (4)) strictly proportional to their average mass, and therefore  $\tau_{1C}$  is strictly comparable to sweeps. Absolute CPU times per spin in our realizations on a Cray X-MP are: 5.8  $\mu$ s and 8.8  $\mu$ s for 1C in  $d=2$  and  $d=3$ , and 6.5  $\mu$ s and 7.6  $\mu$ s for SW with the Hoshen-Kopelman [9] cluster algorithm. Ratios of correlation times in table 1 thus correspond to CPU times within 15%, which, however, clearly depends on details in the programs. In figs. 2 and 3 we see plots of autocorrelation times together with fits for the dynamical exponents  $z$  according to

$$\tau \propto L^z. \quad (15)$$

Data points through which the solid lines pass have been used for the fits, and errors on  $z$  are purely statistical. The small deviations from linear behavior in the log-log plot suggest that our  $z$ -values may be slightly systematically high and should be upper bounds. We realize that our  $z$ 's for SW are somewhat smaller than those quoted in ref. [1]. Since not many details are given there on how these values were obtained we are unable to judge these discrepancies. In ref. [10] a theoretical Ansatz explaining some features of the SW dynamics has been presented. It is interesting to note that it can also accommodate our values for  $z$ . They imply, however, a fractal dimension of typical clusters, whereas SW's own values

Table 1

Results of cluster simulations of the critical Ising model on  $L^d$  lattices. #C is the number of simulated clusters.

$d$	$L$	#C ( $\times 10^{-6}$ )	$E$	$\chi/L^2$	$\tau_{E,1C}$	$\tau_{\chi,1C}$	$\tau_{E,SW}$	$\tau_{\chi,SW}$
2	16	1.02	0.72668(20)	0.5459(5)	1.45(1)	1.22(1)	3.31(4)	3.16(4)
2	32	1.02	0.71684(13)	0.4592(5)	1.80(1)	1.42(1)	4.13(7)	3.78(6)
2	64	0.51	0.71199(12)	0.3860(6)	2.23(3)	1.67(3)	4.92(8)	4.32(8)
2	128	0.54	0.70957(8)	0.3249(6)	2.69(4)	1.84(3)	6.00(8)	4.96(8)
2	256	0.32	0.70827(6)	0.2725(8)	3.17(8)	2.00(6)		
3	16	1.28	0.34504(16)	1.373(4)	1.36(2)	1.01(2)	5.6(1)	5.5(1)
3	24	0.86	0.33842(15)	1.354(7)	1.50(3)	1.06(2)	6.8(1)	6.6(1)
3	32	1.28	0.33562(10)	1.344(7)	1.72(4)	1.14(3)	7.8(3)	7.4(2)
3	48	0.96	0.33333(9)	1.333(10)	1.90(6)	1.20(4)	9.9(4)	9.4(5)
3	64	1.47	0.33210(6)	1.298(9)	1.97(5)	1.20(3)	11.2(5)	11.5(5)

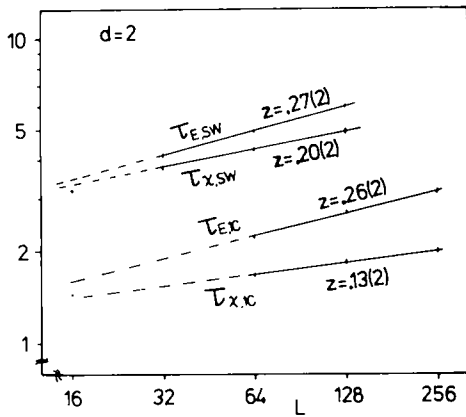


Fig. 2. Integrated autocorrelation times for  $d=2$ .

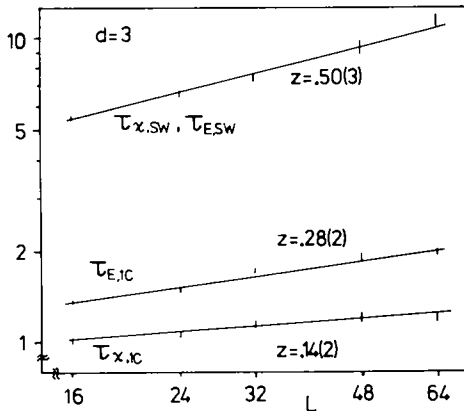


Fig. 3. Integrated autocorrelation times for  $d=3$

point to a dimension close to the geometrical dimension of the underlying space.

We only make a few comments on our results for  $E$  and  $\chi$ . All estimates obtained from both 1C and SW were compatible with each other. Eq. (4) was always found valid as a check<sup>#1</sup>. In two dimensions  $E$  is known exactly for periodic boundary conditions [12], and our results are correct within errors. In  $d=3$  we

<sup>#1</sup> Also the errors in measuring either side of (4) were the same. This shows that improved cluster estimators are no real advantage for the system at criticality. The situation is very different when one measures exponentially decaying correlations at finite correlation length [11,4]

compared with ref. [8] and found agreement<sup>#2</sup>. From  $\chi$  we can fit the critical exponent  $\eta$  in

$$\chi \propto L^{2-\eta}, \tag{16}$$

and we get

$$\begin{aligned} \eta &= 0.2500(7) \quad \text{for } d=2, \\ &= 0.035(4) \quad \text{for } d=3. \end{aligned} \tag{17}$$

This compares favorably with  $\eta = \frac{1}{4}$  ( $d=2$ , exact), and  $\eta$  values in ref. [13] for  $d=3$ .

To conclude: In the Ising model we found the single cluster (1C) algorithm superior to SW updating with a gain that seems to grow with space dimension. Results for  $d=4$  would be of interest. The dynamical exponent  $z$  for long-range quantities like  $\chi$  in  $d=3$  is extremely small and – also very important in practice – the magnitude is such that we see integrated autocorrelation times between one and two only.

The author would like to thank Alan Sokal for an advance copy of ref. [5]. Hospitality of the DESY theory group is acknowledged.

<sup>#2</sup> Although ref. [8] uses helical boundary conditions, we found the expected systematically different finite-size effects invisible for our lattice sizes and statistical accuracy.

References

- [1] R.H. Swendsen and J.-S. Wang, Phys. Rev. Lett. 58 (1987) 86.
- [2] U. Wolff, Phys. Rev. Lett. 62 (1989) 361.
- [3] U. Wolff, DESY report 88-176, to appear in Nucl. Phys. B.
- [4] U. Wolff, DESY report 89-21, Phys. Lett. B 222 (1989) 473
- [5] R.G. Edwards and A. D. Sokal, NYU preprint (May 1989).
- [6] Ch. Frick, K. Jansen and P. Seufferling, HLRZ Jülich preprint 89-38.
- [7] N. Madras and A. D. Sokal, J. Stat. Phys. 50 (1988) 109.
- [8] M.N. Barber, R. B. Pearson, D. Toussaint and J.L. Richardson, Phys. Rev. B 32 (1985) 1720.
- [9] J. Hoshen and R. Kopelman, Phys. Rev. B 14 (1976) 3438
- [10] W. Klein, T. Ray and P. Tamayo, Phys. Rev. Lett. 62 (1989) 163
- [11] U. Wolff, Nucl. Phys. B 300 [FS22] (1988) 501
- [12] B.M. McCoy and T. T. Wu, The two-dimensional Ising model (Harvard U.P. Cambridge, MA, 1973).
- [13] G.S. Pawley, R. H. Swendsen, D.J. Wallace and K. G. Wilson, Phys. Rev. B 29 (1984) 4030